

Inhibitors of epidermal growth factor receptor tyrosine kinase: Optimisation of potency and in vivo pharmacokinetics

Peter Ballard,^a Robert H. Bradbury,^a Craig S. Harris,^b Laurent F. A. Hennequin,^b Mark Hickinson,^a Jason G. Kettle,^{a,*} Jane Kendrew,^a Teresa Klinowska,^a Donald J. Ogilvie,^a Stuart E. Pearson,^a Emma J. Williams^a and Ingrid Wilson^a

^aAstraZeneca, Mereside, Alderley Park, Macclesfield, Cheshire SK10 4TG, UK

^bAstraZeneca, Centre de Recherches, Z.I. la Pompelle, BP1050, 51689 Reims Cedex 2, France

Received 30 May 2006; revised 13 June 2006; accepted 14 June 2006

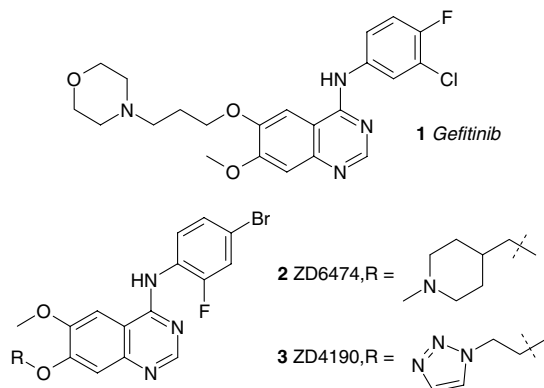
Available online 27 June 2006

Abstract—The structure–activity and structure–property relationships of anilinoquinazoline inhibitors of EGFR were investigated. Strategies to lower volume of distribution and shorten half-life through structure and pK_a modulation are discussed.
© 2006 Elsevier Ltd. All rights reserved.

In recent years, 4-anilinoquinazolines have emerged as a versatile template for inhibition of a diverse range of receptor tyrosine kinases. The most widely studied of these is the epidermal growth factor receptor (EGFR),¹ with the small-molecule inhibitor gefitinib **1**² being the first agent from this class to be approved for the treatment of non-small cell lung cancer refractory to prior chemotherapeutic intervention. Subsequent research aimed at further exploration of the SAR of this novel template has led to compounds that selectively target an array of different kinases, including for example SRC,³ aurora,⁴ the MAP kinase p38 and CDK2.⁵ Our own efforts have also identified ZD6474 **2**,⁶ a highly potent inhibitor of vascular endothelial growth factor (VEGF) Receptor and EGFR that is currently in clinical trials for the treatment of non-small cell lung cancer.⁷

Gefitinib **1** and ZD6474 **2** share the same anilinoquinazoline core, but differ in both the aniline substitution pattern, and the nature and position of the side chains. These basic side chains (gefitinib $pK_a = 7.2$, ZD6474 $pK_a = 9.3$) serve to improve physical properties and confer a favourable pharmacokinetic profile in animals and human. One consequence of the introduction of a basic side chain is to increase the volume of distribution at steady state (V_{dss}), and thus increase the observed

half-life. Whilst a long terminal half-life is desirable in terms of increasing drug exposure and ultimately efficacy, drug accumulation may in theory be an issue, and extended washout times required should therapy need to be discontinued. A detailed DMPK study of gefitinib indicated half-lives of 7–14 h in rat with corresponding $V_{dss} = 8–10$ l/kg.⁸ Mean terminal half-life in healthy volunteers is 28 h (range 12–51 h)⁹ and two separate phase I studies in cancer patients have indicated a mean terminal half-life of 41 h,¹⁰ and 48 h, respectively (range 37–65 h).¹¹ In a comparison between ZD6474 and ZD4190 **3**, an early prototype VEGFR inhibitor, the switch to a basic side chain from a neutral one saw the half-lives increase 12- and 8-fold in rat and dog, respectively.⁶ In a phase I study in 49 cancer patients, the half-life of ZD6474 was found to be approximately 120 h.¹²



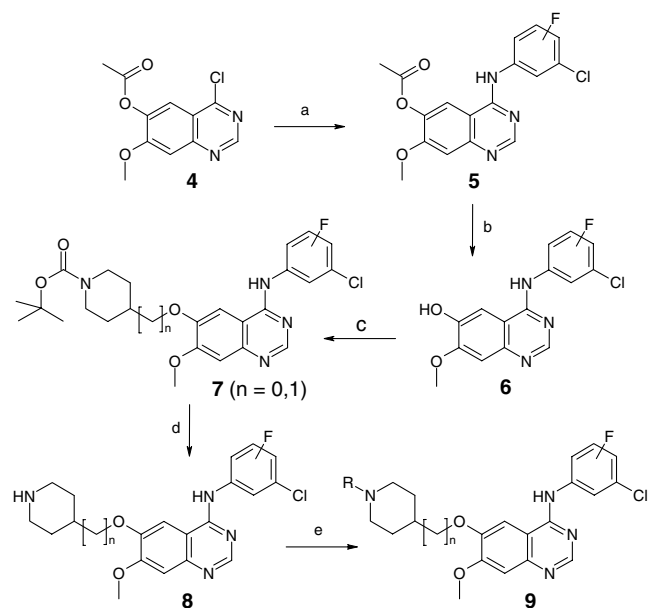
Keywords: EGF; Kinase; Inhibitor; DMPK.

* Corresponding author. Tel.: +44 1625517920; fax: +44 1625586707; e-mail: jason.kettle@astrazeneca.com

Since treatment outcome for many anti-cancer agents is often directly linked with pharmacokinetic exposure¹³ and this exposure can vary substantially between patients, we sought to re-examine the structure–activity relationships of gefitinib analogues, in particular with a view to further optimising potency, and to modulate half-life through direct targeting of V_{dss} . Whilst lowering V_{dss} should have the desired effect of reducing half-life (given a constant clearance), at the outset of this work it was unclear how this strategy would influence physical properties, and critically, the observed *in vivo* efficacy, since effective tissue penetration and duration of effect will still be required at the site of action. Herein we report our preliminary findings.

Aniline variants of gefitinib, **10** and **11**, were synthesised by a procedure analogous to that previously reported.¹⁴ Scheme 1 outlines the generic synthesis of the remaining compounds presented in this study. Accordingly, chloroquinazoline **4**¹⁴ was treated with the requisite fluoro-chloroanilines to give anilinoquinazolines **5**, whose 6-phenol could be unmasked by treatment with ammonia in methanol, to give **6**. Alkylation of **6** with protected side chains was effected under basic conditions, with sulfonate esters derived from the corresponding alcohols to give precursors **7** ($n = 0$ and 1). Cleavage of the side-chain carbamates with TFA to yield N–H piperidines **8** was followed by derivatisation, under appropriate conditions to give target compounds, represented by **9**.

We first examined alternative fluorine regioisomers of **1**, specifically 2-fluoro analogue **10** and 6-fluoro analogue **11** (Table 1). Introduction of the 2-fluoro substituent

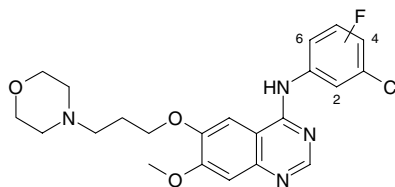


Scheme 1. Generic synthesis scheme for 6-substituted anilinoquinazolines. Reagents and conditions: (a) fluoro-chloroaniline, IPA, reflux; (b) aq NH_3 , MeOH, 50 °C; (c) $n = 0$: R-OMs, CsF, DMA, 85 °C; $n = 1$: R-OTos, K_2CO_3 , DMA, 80 °C; (d) TFA, 25 °C; (e) R = Me: aq formaldehyde, HCO_2H , 90 °C; R = $\text{CH}_2\text{CH}_2\text{OMe}$: K_2CO_3 , DMA, 60 °C; R = CH_2CONH_2 : DIPEA, DCM, 25 °C; R = SO_2Me : DIPEA, DCM, 25 °C.

resulted in a potent inhibitor of EGFR at both enzyme and cellular levels.¹⁵ Interestingly, improvements were seen in both solubility and plasma protein binding (PPB) measurements in both rat and mouse for this seemingly conservative change. The 6-fluoro analogue **11** was in comparison a weaker inhibitor of EGFR, although again showed significant increases in solubility greater than for **10**. Protein binding for **11** was also improved, although in this case slightly inferior to **10** in both species. Table 2 gives selected pharmacokinetic data for these compounds. In the rat, compared to **1**, both **10** and **11** show improved exposure, driven through a combination of lower clearance and improved bioavailability.¹⁶ As a precursor to disease model profiling in mouse xenograft studies, high dose mouse pharmacokinetic studies (po only) were conducted. Again, **10** and **11** showed greater free exposure in the mouse compared to **1**, with **10** in particular showing superior and extended coverage. By the 24 h time-point however plasma levels of **10** and gefitinib **1** were similar, and not detected for **11**.

We next examined alternative side chains in combination with these three anilines. Table 3 indicates potency and physicochemical data for the *N*-methylpiperidin-4-ylmethoxy side chain (designated **A**, as present in ZD6474) and *N*-methylpiperidin-4-yloxy side chain (designated **B**). Compounds **12** and **13** which both contain the 2-fluoroaniline again show potent enzyme and cellular inhibition. In particular, both solubility and rat PPB are improved with side chain **B** compared with side chain **A**. In general, observed solid state melting points for compounds which contained a secondary alkoxide side chain at C-6, such as **B**, were lower than for the corresponding primary alkoxide side chains such as in **A**, which we attribute to less efficient crystal packing. This may contribute in part to the observed physicochemical differences, and it is speculated that a similar phenomenon may be at work with 2-fluoro analogues **10** and **11** where additional twist in the aniline ring in the solid state leads to improved solubility. For 4-fluoro and 6-fluoro analogues with side chains **A** and **B**, activity appears less consistent, with **15** and **17** (which both contain *N*-methylpiperidin-4-yloxy side chain **B**) showing reduced enzyme and cellular activity.

Compounds **12–17** all share relatively basic side chains (*N*-methylpiperidin-4-ylmethoxy side chain **A**, $\text{pK}_a = 9.3$; *N*-methylpiperidin-4-yloxy side chain **B**, $\text{pK}_a = 8.8$) that contribute to the good physicochemical properties observed. However, the expectation was, as discussed above, that this may result in an undesirable pharmacokinetic profile. Table 5 details rat pharmacokinetic data for compound **13**, which shows a very high V_{dss} of 20.8 l/kg consistent with the side-chain basicity, and high plasma clearance and low total plasma levels, despite showing good bioavailability.¹⁷ The solubility and free fraction increments observed by switching to anilines containing a 2-fluoro substituent, as in **10** and **11**, combined with the observations around similar improvements with *N*-methylpiperidin-4-yloxy side chain **B**, led us to target a small array of compounds

Table 1. Potency and physicochemical properties of fluorine regioisomers of gefitinib

Compound		EGFR IC ₅₀ ^a (nM)	KB cell IC ₅₀ ^a (nM)	Solubility ^b (μM)	Rat PPB % free drug ^c	Mouse PPB % free drug ^c
1	4-F	23 ^d	80 ^d	4	3.3	3.0
10	2-F	18 ± 5	21 ± 9	50	7.2	7.5
11	6-F	51 ± 4	110 ± 37	320	5.3	7.3

^a For determinations where $n \geq 2$, standard deviation is given.

^b Aqueous solubility measured in pH 7.4 buffer on pure but generally amorphous material.

^c Measured at 37 °C.

^d See Ref. 14.

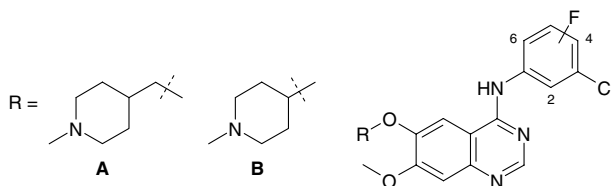
Table 2. In vivo pharmacokinetics of fluorine regioisomers of gefitinib in rodents

Compound		Rat pharmacokinetic profile ^a				Mouse free plasma levels ^b (μM)			
		Bioavailability (%)	Cl (ml/min/kg)	V_{dss} (l/kg)	AUC (po) ^c (μM h)	2 h	4 h	6 h	24 h
1	4-F	56	68	5.8	0.32	0.26	0.13	0.15	0.01
10	2-F	73	29	4.3	0.94	0.43	0.68	0.41	0.01
11	6-F	71	16	3.5	1.64	0.30	0.36	0.17	0

^a From an oral dose of 10 mg/kg, iv dose of 2 mg/kg in Alderley Park—Wistar rats.

^b Following a single oral dose of 50 mg/kg in Alderley Park mice. Free levels calculated on the basis of data in Table 1.

^c Total AUC normalised to a dose of 1 mg/kg.

Table 3. Potency and physicochemical data for anilinoquinazolines 12–17

Compound	Aniline	R	EGFR IC ₅₀ ^a (nM)	KB cell IC ₅₀ ^a (nM)	Solubility ^b (μM)	Rat PPB % free drug ^c
12	2-F	A	2 ± 0	15 ± 6	15	11.2
13	2-F	B	2 ± 2	21 ± 1	130	18.3
14	4-F	A	3 ± 2	18 ± 7	120	2.5
15	4-F	B	10 ± 2	300	100	8.2
16	6-F	A	9 ± 2	58 ± 4	1885	8.6
17	6-F	B	106 ± 15	115 ± 54	—	—

^a For determinations where $n \geq 2$, standard deviation is given.

^b Aqueous solubility measured in pH 7.4 buffer on pure but generally amorphous material.

^c Measured at 37 °C.

based upon reduction of the pK_a in this series. It was anticipated that the likely reduction in solubility and free drug levels through lowering of pK_a could at least in part be ameliorated by these beneficial structural changes. Accordingly, we selected three *N*-substituents to span a range of lowered side-chain basicities, an *N*-methoxyethoxy ($pK_a = 8.1$, compounds **18** and **21**), and *N*-2-acetamide ($pK_a = 6.7$, compounds **19** and **22**) and an *N*-SO₂Me (neutral, compounds **20** and **23**) side chain (Table 4).

As before, compounds containing the 2-fluoro aniline showed greater potency at enzyme and cellular levels than their 6-fluoro counterparts. Activity was fairly consistent across the various *N*-substituents for a given aniline, although the more basic analogues **18** and **21** did show reduced activity, particularly in cells. Compounds **19** and **20** are particularly noteworthy for their very potent inhibition of EGFR in these assays. The examination of the effects on solubility and free fraction for a particular triad in this set is instructive. Free fraction

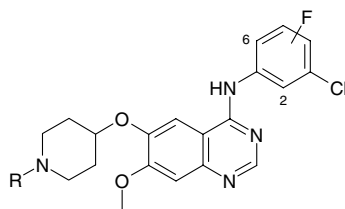
is seen to progressively decrease moving from basic to neutral with both anilines (compare the transition **18** through **20**, and **21** through **23**). A similar effect is seen in solubility for the 6-fluoro analogues **21–23**, where solubility drops from 210 μM for the more basic **21** to 1 μM for the neutral **23**. This effect is not observed with the 2-fluoroanilino analogues **18–20**, where solubility remains modest over the $\text{p}K_{\text{a}}$ range.

Based on the superior potency seen throughout this study with 2-fluoroanilino analogues, and the acceptable physicochemical properties observed with reduced side-chain $\text{p}K_{\text{a}}$ s seen for compounds **18–20** in particular, these compounds were progressed into a rat pharmacokinetic study (Table 5). All three compounds, as anticipated, exhibit a lower V_{dss} relative to the highly

basic close analogue **13**. Bioavailability was observed to be modest, perhaps reflecting solubility limited absorption. Nevertheless, oral exposure was high, as clearance is significantly lowered in this set. Taking all this data together, compound **20** emerged as the best balance of potency, DMPK and physical properties and was selected for further profiling in a mouse LoVo xenograft study. One question regarding the targeting of V_{dss} as a strategy to reduce half-life is the effect on achieving sufficient and extended coverage in disease models. For compound **20**, the observed half-life in rat is 1.6 h, demonstrating the impact of lowering V_{dss} in this series, through targeting of lower $\text{p}K_{\text{a}}$.

We elected to examine **20** in the disease model with both once, and twice daily dosing to examine the

Table 4. Potency and physicochemical data for anilinoquinazolines **18–23**



Compound	Aniline	R	EGFr IC ₅₀ ^a (nM)	KB cell IC ₅₀ ^a (nM)	Solubility ^b (μM)	Rat PPB % free drug ^c
18	2-F	CH ₂ CH ₂ OMe	3 \pm 1	35 \pm 30	3.5	13.4
19	2-F	CH ₂ CONH ₂	2 \pm 1	4 \pm 3	1.7	4.4 ^d
20	2-F	SO ₂ Me	2 \pm 2	7 \pm 4	4	3.3
21	6-F	CH ₂ CH ₂ OMe	114 \pm 1	166	210	9.9
22	6-F	CH ₂ CONH ₂	9 \pm 2	10 \pm 11	8.9	3.1
23	6-F	SO ₂ Me	1 \pm 0	41 \pm 13	1	1.8

^a For determinations where $n \geq 2$, standard deviation is given.

^b Aqueous solubility measured in pH 7.4 buffer on pure but generally amorphous material.

^c Measured at 37 °C.

^d Measured at 25 °C.

Table 5. Selected rat pharmacokinetic data^a for anilinoquinazolines **13**, and **18–20**

Compound	R	Side-chain $\text{p}K_{\text{a}}$	Bioavailability (%)	Cl (ml/min/kg)	V_{dss} (l/kg)	AUC (po) ^b ($\mu\text{M h}$)
13	Me	8.8	74	129	20.8	0.08
18	CH ₂ CH ₂ OMe	8.1	30	11	1.3	0.95
19	CH ₂ CONH ₂	6.7	27	16	2.7	0.59
20	SO ₂ Me	—	45	13	1.5	1.18

^a From an oral dose of 5 mg/kg, iv dose of 2 mg/kg in Alderley Park—Wistar rats.

^b Total AUC normalised to a dose of 1 mg/kg.

Table 6. Comparison of xenograft data for compounds **1** and **20**

Compound	Dose (mg/kg)	Inhibition of tumour volume ^a (%)	Significance (P value)	AUC (po) ^c ($\mu\text{M h}$)	C_{max} ^c (μM)
1	50	60	0.018	78.7	8.1
1	100	84	0.002	85.9	6.7
20	50	53	0.018	224.9	30.6
20	100	60	0.011	450.5	36.8
20 ^b	2 \times 50	91	<0.001	286.3	23.9

^a Inhibition of tumour volume relative to control group measured at day 17.

^b Doses separated by 12 h.

^c Exposure observed in xenograft study.

impact of these changes. Female nude mice were implanted subcutaneously with 1×10^7 LoVo colon tumour cells. Once tumours were established, animals were randomised between groups ($n = 7$ per group) and dosed po with compound suspended in 1% (v/v) polysorbate 80. Table 6 indicates the efficacy and exposure of compound **20** in this study, alongside **1** for comparative purposes. As expected, gefitinib **1** shows good activity and clear dose–response at 50 and 100 mg/kg doses. Compound **20** shows comparable activity at 50 mg/kg, although appears less efficacious at the higher dose of 100 mg/kg, despite linear increases in exposure over the dose range. However, consistent with the shorter half-life for this compound, dosing twice a day results in 91% inhibition of tumour volume relative to control animals, substantially better than once a day dosing, including at 100 mg/kg.

In summary, in the compounds tested aniline and side-chain structural modifications to the EGFR inhibitory anilinoquinazoline template gave substantial increases in enzyme and cellular potencies. These changes in combination with side-chain pK_a modulation have led to compounds with a markedly altered pharmacokinetic profile, which nevertheless show profound inhibition of tumour growth in a selected disease model.

References and notes

1. Hynes, N. E.; Lane, H. A. *Nat. Rev. Cancer* **2005**, *5*, 341.
2. Cohen, M. H.; Williams, G. A.; Sridhara, R.; Chen, G.; McGuinn, W. D., Jr.; Morse, D.; Abraham, S.; Rahman, A.; Liang, C.; Lostritto, R.; Baird, A.; Pazdur, R. *Clin. Cancer Res.* **2004**, *10*, 1212.
3. Ple, P. A.; Green, T. P.; Hennequin, L. F.; Curwen, J.; Fennell, M.; Allen, J.; Lambert-van der Brempt, C.; Costello, G. *J. Med. Chem.* **2004**, *47*, 871.
4. Mortlock, A. A.; Keen, N. J.; Jung, F. H.; Brewster, A. G. PCT Int. Appl. WO 2001021596.
5. Shewchuk, L.; Hassell, A.; Wisely, B.; Rocque, W.; Holmes, W.; Veal, J.; Kuyper, L. F. *J. Med. Chem.* **2000**, *43*, 133.
6. Hennequin, L. F.; Stokes, E. S. E.; Thomas, A. P.; Johnstone, C.; Plé, P. A.; Ogilvie, D. J.; Dukes, M.; Wedge, S. R.; Kendrew, J.; Curwen, J. O. *J. Med. Chem.* **2002**, *45*, 1300.
7. Heymach, J. V. *Br. J. Cancer* **2005**, *92*(Suppl.1), S14.
8. McKillop, D.; Partridge, E. A.; Hutchison, M.; Rhead, S. A.; Parry, A. C.; Bardsley, J.; Woodman, H. M.; Swaisland, H. C. *Xenobiotica* **2004**, *34*, 901.
9. Swaisland, H.; Laight, A.; Stafford, L.; Jones, H.; Morris, C.; Dane, A.; Yates, R. *Clin. Pharmacokinetics*. **2001**, *40*, 297.
10. Tiseo, M.; Loprevite, M.; Ardizzoni, A. *Curr. Med. Chem.—Anti-Cancer Agents* **2004**, *4*, 139.
11. Ranson, M.; Hammond, L. A.; Ferry, D.; Kris, M.; Tullo, A.; Murray, P. I.; Miller, V.; Averbuch, S.; Ochs, J.; Morris, C.; Feyereislova, A.; Swaisland, H.; Rowinsky, E. K. *J. Clin. Oncol.* **2002**, *20*, 2240.
12. Miller, K. D.; Trigo, J. M.; Wheeler, C.; Barge, A.; Rowbottom, J.; Sledge, G.; Baselga, J. *Clin. Cancer Res.* **2005**, *11*, 3369.
13. Undevia, S. D.; Gomez-Abuin, G.; Ratain, M. J. *Nat. Rev. Cancer* **2005**, *5*, 447.
14. Barker, A. J.; Gibson, K. H.; Grundy, W.; Godfrey, A. A.; Barlow, J. J.; Healy, M. P.; Woodburn, J. R.; Ashton, S. E.; Curry, B. J.; Scarlett, L.; Henthorn, L.; Richards, L. *Bioorg. Med. Chem. Lett.* **2001**, *11*, 1911.
15. Compounds were evaluated in an EGFR kinase assay measuring inhibition of phosphorylation of a synthetic peptide substrate at K_m ATP concentration. Inhibition of proliferation of KB cells in response to EGF stimulus was also assessed. For details of assay conditions see, Hennequin, L. F. A.; Kettle, J. G.; Pass, M.; Bradbury, R. H. PCT Int. Appl. WO2003040109.
16. The rat pharmacokinetic data reported in this paper are from a protocol designed to allow high throughput profiling of compounds and as such are non-optimised. Literature data for **1** (see Ref. 8) show some variance with the data in Table 2 due to the more detailed nature, and differing protocols used in these studies.
17. While the clearance figure of 129 ml/min/kg is seemingly at odds with the reported bioavailability of 74%, it should be noted that this is for clearance of drug from plasma. This basic compound partitions extensively into blood, such that the blood clearance is a more realistic 65 ml/min/kg. Nevertheless, the good bioavailability observed may reflect saturation of first-pass clearance, or other non-hepatic routes of elimination.